Effects of A/B cation ratio on the microstructure and lifetime of $(Ba_{1-x}Ca_x)_z(Ti_{0.99-y}Zr_yMn_{0.01})O_3$ (BCTZM) sintered in reducing atmosphere

WEN-HSI LEE, TSEUNG-YUEN TSENG
Department of Electronics Engineering and Institute of Electronics, National Chiao-Tung University, Hsinchu, Taiwan
E-mail: tseng@cc.nctu.edu.tw

D. HENNINGS
Philips Research Laboratory Aachen, 5100 Aachen, Germany

Microstructure and dielectric properties of $(Ba_{1-x}Ca_x)_z(Ti_{0.99-y}Zr_yMn_{0.01})O_3$ (BCTZM) with various cation ratios (A/B) sintered in reducing atmosphere and then annealed to reoxidize the ceramic bodies were investigated. With decreasing A/B cation ratio, concurrent with the grain size reduction, the insulation resistance and lifetime of the BCTZM are both increased. The degradation of insulation resistance is closely related to oxygen partial pressure used during annealing and the resulting microstructure of the ceramics. Within the same volume, the specimen with fine grain size provides more grain boundaries, in comparison to large grain size specimens, which helps in providing an efficient diffusion pathway for oxygen during annealing. The result of oxidation of the Mn, that is, a change in the valence state of Mn from Mn^{+2} to Mn^{+3} is confirmed from thermogravimetric analysis and electron paramagnetic resonance analysis.

1. Introduction

High-permittivity $(Ba,Ca)(Ti,Zr)O_3$ dielectric ceramics doped with acceptor-type additives have been studied to produce reliable Ni-electrode multilayer ceramic chip capacitors (MLCCs) [1]. To avoid oxidation of the Ni electrodes, the capacitors were sintered in a reducing atmosphere and then annealed to reoxidize the ceramics. Nevertheless, MLCCs still have the weakness of short life, that is, the degradation problem needs to be overcome.

The dielectric properties and degradation of $BaTiO_3$-based dielectrics are sensitively dependent on various factors such as A/B ratio, the amount of additive and nature of the sintering atmosphere [2]. For Ti-rich $BaTiO_3$ material, the A/B ratio in the $BaTiO_3$ is one of the important factors which has been known to dramatically influence the microstructural development due to the existence of excess TiO_2 which forms a eutectic liquid phase with $BaTiO_3$ at 1332 °C [3]. The presence of Ti-rich second phase $Ba_6Ti_{17}O_{40}$ in samples with A/B ratio higher than unity led to degradation of the insulation resistance at high temperature. This degradation phenomenon was interpreted as an influence of grain size in terms of the grain-boundary model [4].

In the present work, the influence of small changes in A/B ratio on the insulation resistance and lifetime of $(Ba_{1-x}Ca_x)_z(Ti_{1-y}Zr_yMn_{0.01})O_3$ (BCTZM) samples were investigated. In addition, we attempted to understand the relation between lifetime and A/B non-stoichiometry ratio from microstructure and reoxidation mechanisms. We also studied the influence of grain size on the degradation of BCTZM samples.

2. Experimental

The samples were prepared from high purity $BaCO_3$ (Nippon-Chemical), TiO_2 (Fuji Titanium), $CaCO_3$ (Merck), ZrO_2 (Merck) and MnO_2 (Merck) raw materials by using the conventional solid state reaction method. The raw materials were weighed according to the chemical formula $(Ba_{1-x}Ca_x)_z(Ti_{0.99-y}Zr_yMn_{0.01})O_3$ with x fixed at 0.13 and y ranging from 0.140 to 0.132 in steps of 0.002 and z ranging from 0.993 to 0.999 in steps of 0.002. The cation ratio of A-site ions (Ba, Ca) and B-site ions (Ti, Zr, Mn) was carefully controlled and checked by using X-ray fluorescence. Samples with A/B ratios of 0.993, 0.995, 0.997 and 0.999 were employed.

All batches were wet ball-milled in a polypropylene bottle, dried and calcined at a temperature of 1000 °C for 4 h in a pure alumina crucible. Milling of calcined powders to an average particle size of 1 μm was carried out. These powders were pressed into discs with a diameter of 10 mm. Ceramic disks were then sintered at a temperature of 1300 °C for 4 h in a moist reducing atmosphere $(P_{O_2} = 1.183 \times 10^{-10}\,Pa)$ which was controlled by the equilibrium of H_2 and H_2O. Subsequently, annealing in an oxygen partial pressure below $1.7 \times 10^{-6}\,Pa$ at 1000 °C was carried out to reoxidize the ceramic bodies. The annealed samples were polished and electroded with Dupont 7095 silver paste.

Dilatometry was used to observe the whole procedure of the densification of ceramic disks sintered in flowing wet forming gas (95/5 N_2/H_2). The procedure for the dilatometry was as follows: heating at $2\,°C\,min^{-1}$, to $1300\,°C$, followed by an isothermal hold for 1 h and then cooling at $10\,°C\,min^{-1}$ to $300\,°C$.

The Archimedean method was employed for density measurement using deionized water as the immersion liquid. The microstructures of polished samples were examined by scanning electron microscopy (SEM, model S2500, Hitachi, Tokyo, Japan). The grain size was estimated by the linear intercept technique.

In this paper, experimental data represent multiple measurements on ten specimens. The insulation resistance was measured with a Hewlett-Packard (HP) 4140A at d.c. voltage of 50 V for 2 min. The life stability of dielectric materials was commonly evaluated from extended measurements of the insulation resistance (IR) under electric field and temperature stress. Highly accelerated life test (HALT) experiments on ceramic disks with 400–450 µm thickness were performed at $140\,°C/200\,V$.

Reoxidation kinetics of the samples with dimensions of $3 \times 3 \times 10$ mm were examined by mean of thermogravimetric isothermal analysis (TGA). The weight changes due to annealing in atmospheres of various oxygen partial pressures were determined. Electron paramagnetic resonance spectra (EPR, Bruker EMX-10, X-band, 9.776 GHz) were recorded at room temperature.

3. Results and discussion

Fig. 1 illustrates the change in shrinkage for BCTZM with various A/B ratios at the same temperature-time profile. Increasing the amount of excess TiO_2 lowered the onset temperature of shrinkage and promoted the densification rate. It is well known that a small excess of TiO_2 reacts with $BaTiO_3$ and forms $Ba_6Ti_{17}O_{40}$, which remains as a eutectic, melts at $1320\,°C$. Therefore, it has been noted that liquid phase sintering occurred at temperatures above the eutectic point, and the rapid grain growth was observed due to the existence of the liquid phase [5]. Fig. 2 shows the relationship between sintered density and A/B ratio of BCTZM. Density increased with decreasing A/B ratio which is attributed to
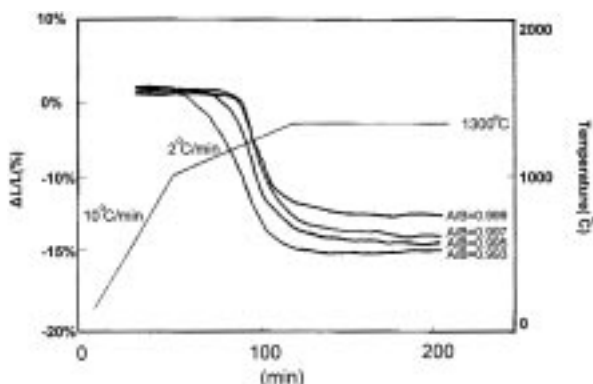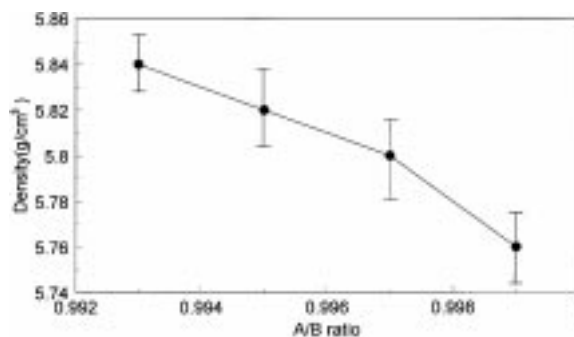

Figure 2 Sintered density of BCTZM as a function of A/B ratio.

the presence of a Ti-rich second phase which has enhanced the densification rate at a temperature above the eutectic point; this is similar to the previously reported results [6].

Fig. 3 shows the SEM microstructures of BCTZM with A/B ratios of 0.999, 0.997, 0.995 and 0.993, respectively. Apparently, a small variation in non-stoichiometry of the order of 0.001 has resulted in a significant change in the grain growth behavior in BCTZM sintered in a reducing atmosphere. The average grain size of BCTZM continuously decreases from 8.1 to 4.9 µm with increasing A/B ratio from 0.993 to 0.999, as shown in Fig. 4.

As shown in Fig. 5, the insulation resistance of BCTZM is approximately inversely proportional to grain size. The insulation resistance at room temperature shows a progressive increase as the grain size is decreased. The insulation resistance is increased from 9.87×10^{10} to $55.7 \times 10^{10}\,\Omega$ when the grain size is decreased from 8.1 to 4.9 µm. The high insulation resistance is mainly caused by the fact that grain boundaries in the dielectric ceramic act as highly resistive barriers for cross-transport of charge carriers. The conduction is of a mixed electronic–ionic nature because electrons and oxygen vacancies act as mobile carriers.

The dependence of insulation resistance of BCTZM on temperature and activation energy (E_a) can be written in the form:

$$IR = A \exp(E_a/kT)$$

The above equation can be described as

$$\ln(IR) = A + E_a/kT$$

where A is a constant related to the composition and structure of the material. From the slope of $\ln(IR)$ versus $1/T$ plot, we can obtain the activation energy. It should be noted that E_a does not always remain constant over the entire temperature range of interest but may vary due to a transition between charge carrier transport regimes. In polycrystalline barium titanate, besides the electronic conduction, ionic (cations, or anions and their vacancies) conduction via motion of oxygen vacancies can also be a major charge transport mechanism [7]. In the present study, the samples exhibit a decrease in electrical resistivity with increasing temperature in the temperatures range from $125\,°C$ to $300\,°C$, as shown in Fig. 6. There is a change in activation energy with A/B ratio of the samples. The activation energies are 0.48, 0.57, 0.64

Figure 1 Shrinkage curves of BCTZM with various A/B ratios sintered at the same temperature-time profile indicated.
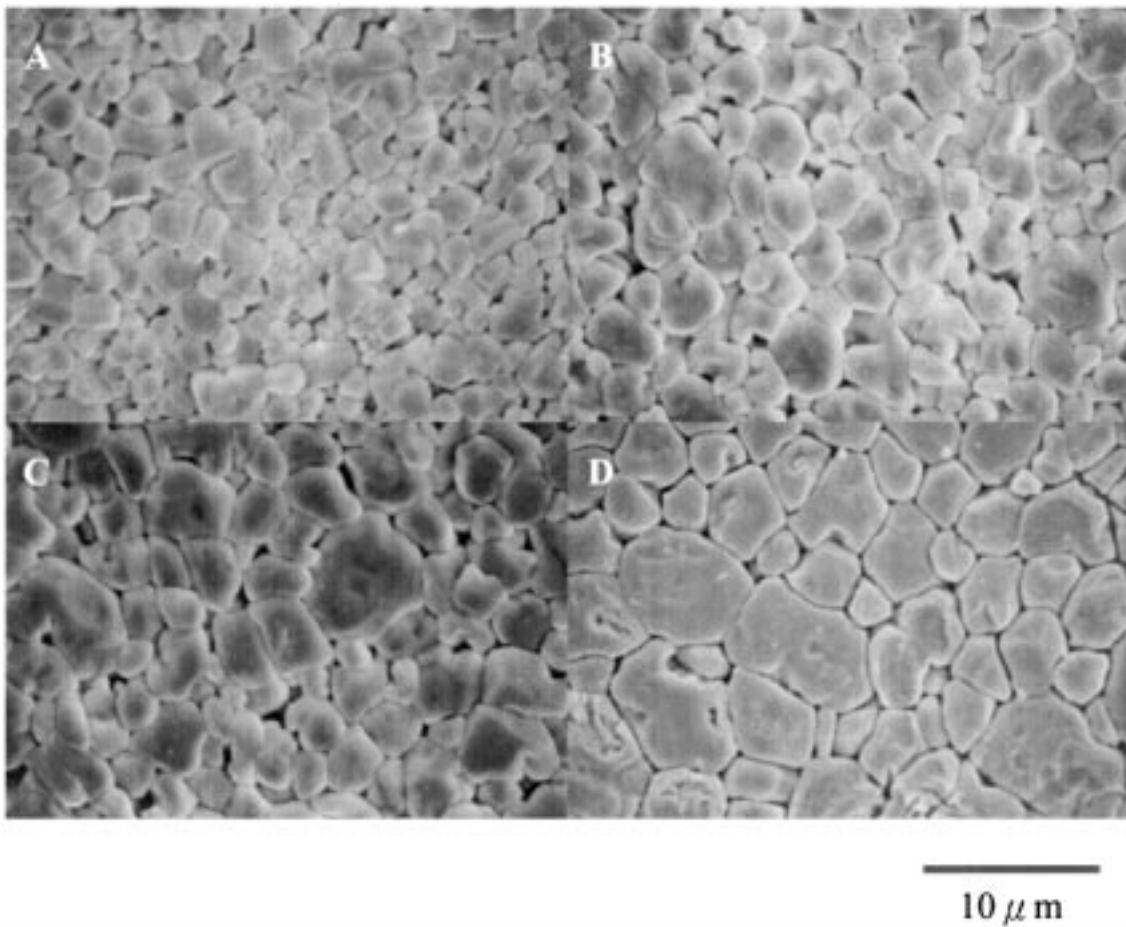
Figure 3 SEM micrographs for BCTZM samples with A/B ratio of (A) 0.999, (B) 0.997, (C) 0.995 and (D) 0.993.
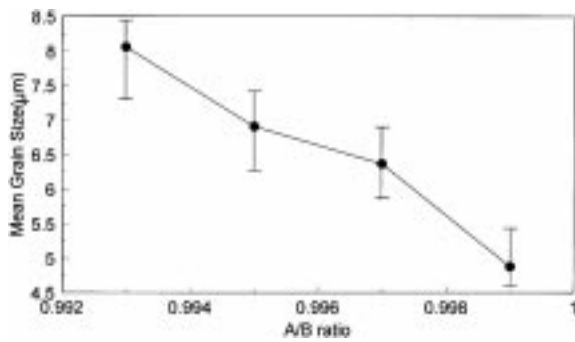

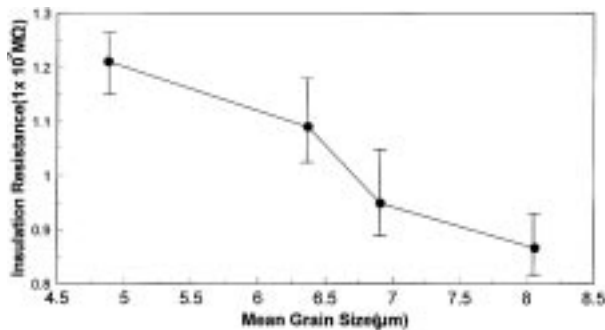*Figure 4* Relationship between mean grain size and A/B ratio for BCTZM samples.

Figure 5 Relationship between insulation resistance and mean grain size for BCTZM samples.

Figure 6 Insulation resistance as a function of reciprocal temperature for various A/B ratio BCTZM samples.

and 0.80 eV for 0.999, 0.997, 0.995 and 0.993 A/B ratios, respectively

The resistivity was found to decrease by decreasing the A/B ratio and by increasing the grain size. In the case of A/B = 0.999, the IR obeys the Arrehenius relationship with an activation energy of approximately 0.48 eV. We believe that the activation energy is mainly due to electronic conduction, which is a thermally activated process resulting from the charge hopping among Mn ions $(Mn^{+2} \rightarrow Mn^{+3} + e^{-})$. Small polaron transport can often be expected from the doping of transition metal
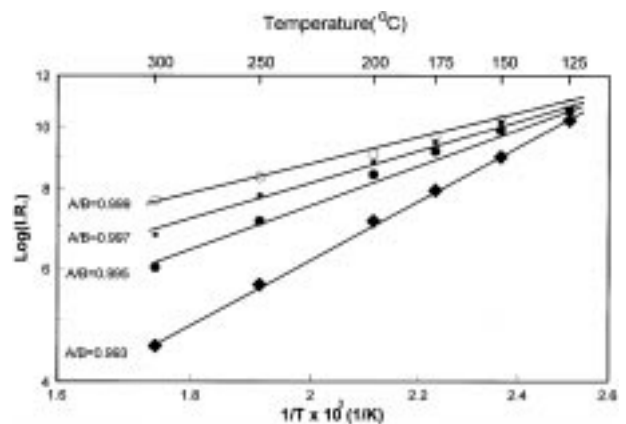
159

cations, giving hopping energies in the range of 0.1 to 0.4 eV [8]. However, for the A/B = 0.993 specimen, there is a maximum activation energy of 0.8 eV as obtained from the specimen with small grain size. This value is close to 0.96 eV reported by Minford [9] as due to the diffusion of oxygen vacancies in polycrystalline barium titanate. The ionic migration energies have been reported to be at least of the order of 0.8 eV or higher [10, 11]. It is suggested that the majority of electrical conductivity for specimens with small A/B ratio is possibly contributed by oxygen vacancies (ionic conduction).

Fig. 7 shows the variation of insulation resistance with time for the samples annealed at $P_{O_2} = 1.7 \times 10^{-6}$ Pa, $P_{O_2} = 2.2 \times 10^{-7}$ Pa, $P_{O_2} = 3.1 \times 10^{-8}$ Pa, and $P_{O_2} = 3.2 \times 10^{-9}$ Pa, respectively. Apparently, oxygen partial pressure also has a strong influence on the IR degradation. The same A/B ratio samples annealed at higher oxygen partial pressure are expected to eliminate more oxygen vacancies, therefore, they have longer lifetime as shown in Fig. 7. On the other hand, the longer lifetime is also observed in the larger A/B ratio samples annealed at the same oxygen partial pressure. Two kinds of possible path for compensation of oxygen during annealing can be proposed as the following:

1. The grain boundary provides a rapid diffusion path for oxygen. Oxygen diffusion starts from a grain boundary into a grain. The diffusion rate is thus grain-size dependent. At the same oxygen partial pressure annealing, the large A/B ratio samples have smaller grain size and larger amounts of grain boundary, consequently,

those samples have more oxygen paths along the grain boundary.

2. The open pores can act as rapid diffusion paths of oxygen for oxidizing the grain boundary. According to previous studies [12, 13], generally, when the sintered density reaches about 92–93% of theoretical density, all pores in the specimen can be closed. In other words, open pores may be present when the total porosity is more than 7–8%. In our experiment, the relative sintered densities for BCTZM with A/B ratio of 0.993, 0.995, 0.997 and 0.999, respectively, reach 99.8%, 99.5%, 99.2% and 98.5%. Therefore, it is assumed that our specimens have only closed pores indicating that grain boundary is the main diffusion path for oxygen during annealing in this study.

The influence of the two mutually interrelated parameters, oxygen partial pressure and grain size, on the degradation rate of IR is illustrated in Fig. 8. Two conclusions can be drawn from the above results:

1. At the same grain size, the samples annealed at higher oxygen partial pressure after sintering effectively increase their insulation resistances and prolong their lifetimes because the larger amount of oxygen vacancies formed in the reducing atmosphere sintering can be compensated during annealing. As shown in a previous report [14], the longer lifetime has been obtained when the higher oxygen partial pressure was used during annealing

2. At the same oxygen partial pressure used during annealing, the smaller grain size provides more grain boundaries which act as diffusion pathways for oxygen, and is also effective to prolong the lifetime of the sample.
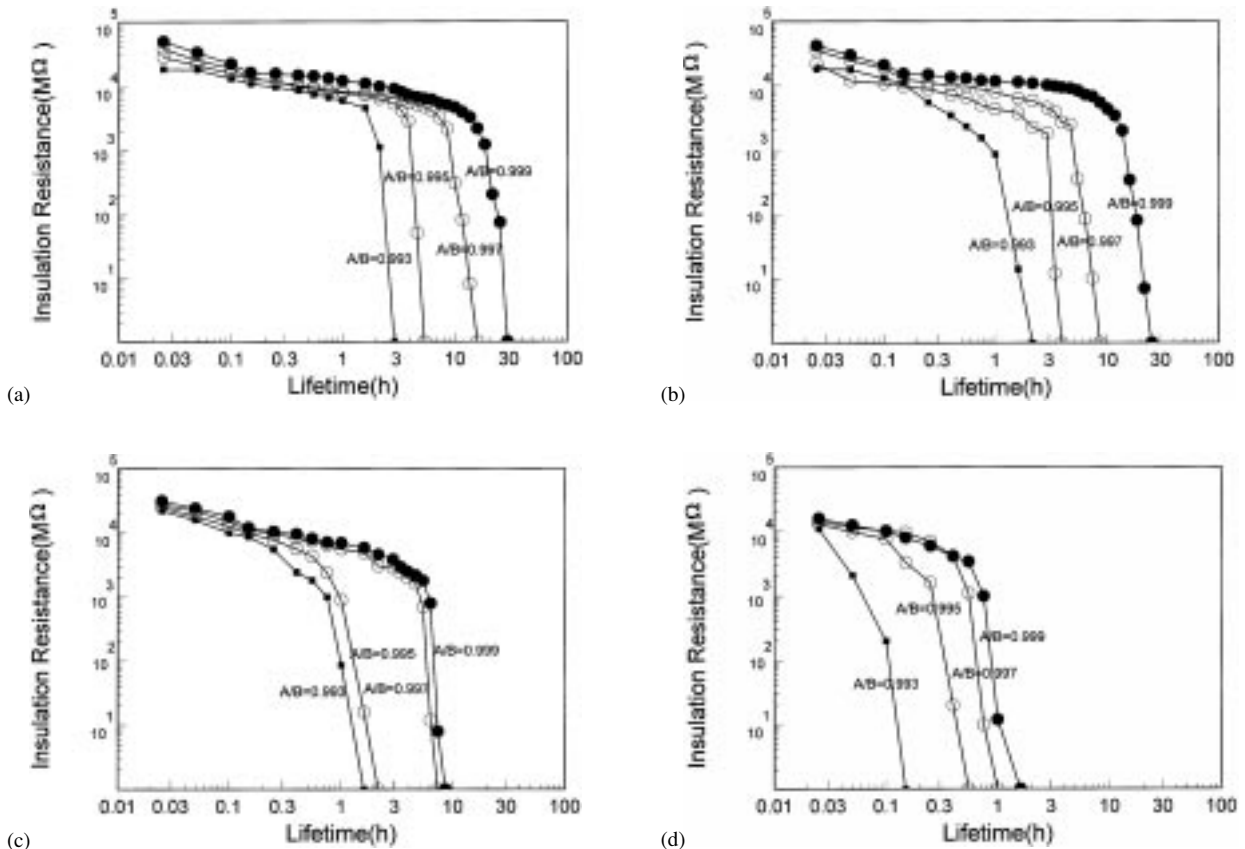

(a)

(b)

(c)

(d)

Figure 7 Variation of insulation resistance against 20 V μm^{-1} at 140 °C with time for BCTZM samples annealed at various P_{O_2} (a) 1.7×10^{-6} Pa, (b) 2.2×10^{-7} Pa, (c) 3.1×10^{-8} Pa and (d) 3.2×10^{-9} Pa.
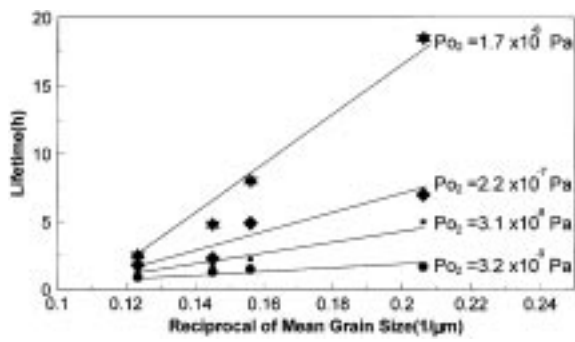
Figure 8 Lifetime as a function of mean grain size for BCTZM with various A/B ratios annealed in various oxygen partial pressures at 1000 °C for 3 h.

Figure 9 Formation of Mn^{+3} as a function of mean grain size for BCTZM with various A/B ratios annealed at various oxygen partial pressures at 1000 °C for 3 h.

The above results have generally been attributed to oxygen adsorption along the grain boundaries and diffusion into the grain interior, altering the defect structure such as diminishing oxygen vacancies or changing the valence of manganese [15, 16]. Mn ions with charge less than $4+$, substitutionally accommodated at Ti sites, act as electron acceptors which are virtually immobile below the temperature of lattice formation. These acceptors neutralize the donor action of oxygen vacancies as follows:

$$O_o \rightarrow 1/2\,O_2 + Vo^{\cdot\cdot} + 2e'$$
$$2Mn^{+2} + V_o^{\cdot\cdot} + 1/2\,O_2 \longrightarrow 2Mn^{+3}$$
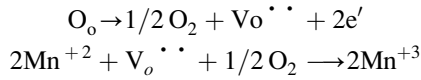
In order to verify the effect of the above reoxidation assumption on the microstructure of BCTZM, examination of the valence of the Mn is necessary. Therefore, the detection of change in the oxidation states of Mn in the samples annealed in various oxygen partial pressures was carried out by using TGA and EPR in the present study.

The oxygen partial pressure for reoxidation of Mn^{+2} into Mn^{+3} is expected to terminate at $P_{O_2} < 5 \times 10^{-6}$ Pa, where the competitive oxidation of the Ni inner electrode begins in 4.7×10^{-6} Pa at 1000 °C. To verify that more effective reoxidation occurred on the BCTZ with smaller grain size due to the existence of more reoxidation channels under the identical area, four kinds of reoxidation atmosphere ($< 5 \times 10^{-6}$ Pa) were conducted for BCTZM with different grain size to evaluate the formation of Mn^{+2} converted into Mn^{+3} through oxygen consumption in TGA measurements. Fig. 9 shows the formation of Mn^{+3} as a function of reciprocal mean grain size under various P_{O_2} annealing. The formation of Mn^{+3} is increased with decreasing grain size for all four kinds of reoxidation atmosphere.

As expected, the more effective reoxidation, and more formation of Mn^{+3}, was revealed on annealing at high oxygen partial pressure. Under $P_{O_2} = 1.7 \times 10^{-6}$ Pa annealing, 100%, 66%, 45% and 25% Mn^{+2} were, respectively, converted into Mn^{+3} for BCTZM with grain sizes 4.9, 6.4, 6.9 and 8.1 μm. The measurements of valence of Mn for BCTZM with various grain sizes using TGA are in accordance with the results of lifetime, as indicated in Fig. 8.

When the same annealing condition was conducted on various A/B ratio samples with approximately the same density, the large difference in lifetime between these samples with various A/B ratios can be explained through the difference of grain size. For the same area,
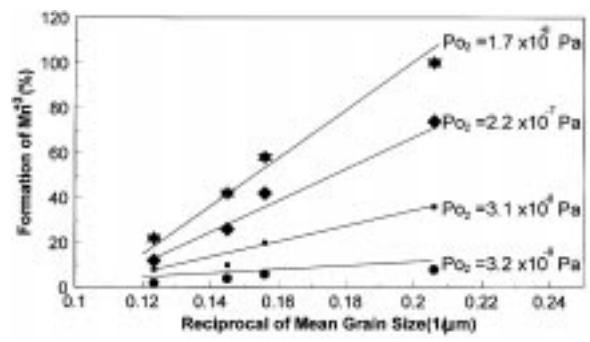
more grain boundaries, which presumably act as diffusive paths of oxygen during annealing, are present for smaller grain size samples in comparison to larger grain size samples. Hence, larger amounts of Mn^{+2} ions changing to Mn^{+3} in small grain size BCTZM during annealing is beneficial to prolong lifetime. In order to further verify this phenomenon, EPR examination of the valence of Mn ions in BCTZM with different A/B ratios was employed. As indicated in Fig. 10, the spectra of A/B = 0.993 correspond to the Lande g-factor of 2.0024 and show the presence of Mn^{+2}. These spectra show the signals of six hyperfine peaks were weakened with increasing A/B ratio. As reported in the previous studies [17, 18], Mn^{+2} and Mn^{+4} resonance can be observed in $BaTiO_3$-based ceramic, whereas Mn^{+3} resonance can be observed only at temperatures below 10 K because of its shorter relaxation time. Consequently, the valence state of Mn would be assumed to more to $+3$ from $+2$ with increasing A/B ratio on the basis of weakened EPR
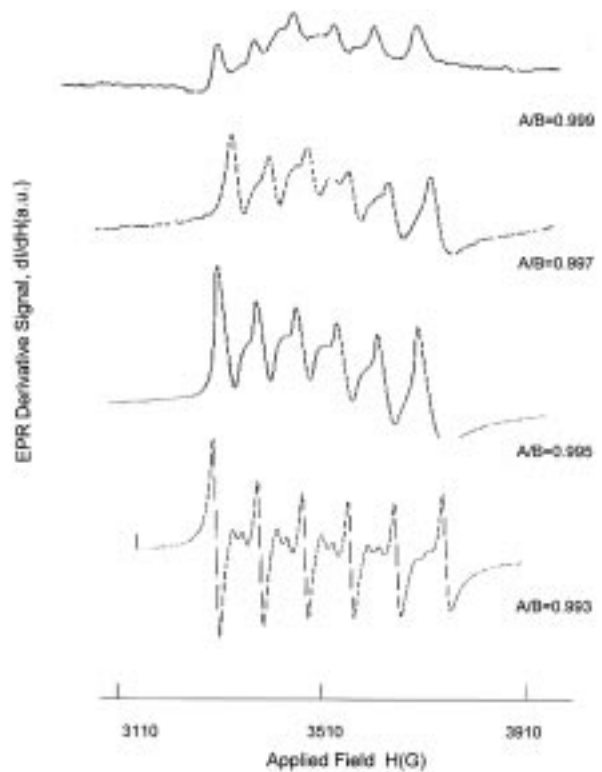

Figure 10 EPR spectra of the samples with various A/B ratios measured at room temperature and from 3110 G to 3910 G (mid. range 3510 G). The instrumental parameters are microwave frequency 9.776 GHz, microwave power 20.0 mW, and gain 10^6.

Mn^{+2} signal of six hyperfine peaks. The results of EPR spectra for different A/B ratios also successfully demonstrated the fact that reoxidation for small grain size samples (i.e., high A/B ratio) is easier than larger grain size samples (i.e., small A/B ratio) due to the difference in the number of grain boundaries which helps in the active diffusion of oxygen. The measurements of valence of Mn by EPR on BCTZM with various grain sizes have demonstrated a good agreement with the TGA results.

Therefore, degradation of insulation resistance is closely related to oxygen partial pressure in annealing and microstructure of BCTZM in this study. The fine grain size provided more grain boundaries, which helps in oxygen diffusion during annealing which is confirmed by detection of conversion of valence of Mn from $+2$ to $+3$ with TGA and EPR.

4. Conclusions

1. The onset temperature of shrinkage is lowered, densification rate is promoted and grain growth is enhanced with increasing TiO_2 excess in BCTZM sintered in a reducing atmosphere and at the same temperature profile. The grain size is decreased from 8.1 to 4.9 μm with increasing A/B ratio from 0.993 to 0.999. Concurrent with the grain size reduction, the insulation resistance and lifetime are both increased.

2. Lifetime is increased with decreasing grain size and is approximately proportional to the reciprocal of grain size which represents the number of grain boundaries which acted as the diffusion path of oxygen. The lifetime is determined by compensation of oxygen to eliminate oxygen vacancies related to the oxygen partial pressure used in annealing.

3. The proportion of conversion of divalent Mn ions into trivalent Mn ions during annealing is closely related to grain size in BCTZM and oxygen partial pressure. Both TGA and EPR measurements were carried out to confirm this phenomenon.

References

1. I. BURN, ''Ceramic Disk Capacitor with Base-Metal Electrodes'', Presented at 1976 Pacific Coast Regional Meeting of the American Ceramic Society San Francisco, California, Nov. 2 (No. 99-BEN-76P).
2. T. YAMAMOTO, *Br. Ceram. Trans.* (1995) 196.
3. J. S. CHOI and H. G. KIM, ''Influence of TiO_2 Excess on the Sintering Behavior and Abnormal Grain Growth of Barium Titanate Ceramics'', Proceedings of the Third International Conference on Properties and Application of Dielectric Materials, July 8–12, Tokyo, Japan (1991).
4. S. SUMITA, M. LKEDA, Y. NAKANO, K. NISHYAMA and T. NOMURA, *J. Am Ceram. Soc.* **74** (1991) 2379.
5. D. T. D. HENNINGS, R. JANNSEN and P. J. L. REYNE, *ibid.* **70** (1987) 23.
6. M. DEMARTIN, G. HERARD, C. CARRY and J. LEMAITRE, *ibid.* **80** (1997) 1079.
7. D. D. GLOWER and R. C. HECKMAN, *J. Chem. Phys.* **41** (9164) 877.
8. S. SATO, Y. NAKANO, A. SATO and T. NOMU, *Jpn. J. Appl. Phys. Part(I)* **9B** (1997) 6016.
9. N. J. MINFORD, *IEEE Trans. Compon Hybrids Manuf., Technol.* **CHMT-5** (9182) 297.
10. H. IHRIG, *J. Phys. C.* **9** (1976) 3469.
11. W. KOFSTAD, ''Nonstoichiometry, Diffusion, and Electrical Conductivity in Binary Metal Oxides'' (John Wiley & Sons, Inc., New York, 1972).
12. D. W. BUDWORTH, *Trans. Br. Ceram. Soc.* **69** (1970) 29.
13. M. KUWABARA, *J. Am. Ceram. Soc.* **64** (1981) 639.
14. J. YAMAMATSU, N. KAWANO, T. ARASHI, A. SATO, Y. NAKANO and T. NOMURA, *J. Powder Source* **60** (1996) 199.
15. H. J. HAGEMANN and H. IHRIG, *Bull. Am. Phys. Soc.* **20** (1979) 3871.
16. I. C. HO and S. L. FU, *J. Am. Ceram. Soc.* **75** (1992) 728.
17. J. H. LEE, S. H. KIM and S. H. CHO, *ibid.* **78** (1995) 2845.
18. P. REN and S. ISHIDA, *J. Ceram. Soc. Jpn.* **103** (1995) 759.